International Journal of Fracture **84:** 191–202, 1997.

Three-dimensional crack problem analysis using boundary element method with finite-part integrals

T.Y. QIN[1], W.J. CHEN[2] and R.J. TANG[3]
[1]*Department of Engineering Basic Sciences, China Agricultural University, Beijing 100083, China*
[2]*Institute of Mechanics, Chinese Academy of Sciences, Beijing 100080,China*
[3]*Department of Engineering Mechanics, Shanghai Jiao Tong University, Shanghai 200030, China*

Received 23 August 1996; accepted in revised form 17 January 1997

Abstract. A set of hypersingular integral equations of a three-dimensional finite elastic solid with an embedded planar crack subjected to arbitrary loads is derived. Then a new numerical method for these equations is proposed by using the boundary element method combined with the finite-part integral method. According to the analytical theory of the hypersingular integral equations of planar crack problems, the square root models of the displacement discontinuities in elements near the crack front are applied, and thus the stress intensity factors can be directly calculated from these. Finally, the stress intensity factor solutions to several typical planar crack problems in a finite body are evaluated.

Key words: planar crack, boundary element method, finite-part integral, hypersingular integral equation, three-dimensional finite body, square root model.

1. Introduction

The investigation of three-dimensional crack problems is very important in practice. Since analytical solutions to these problems have been limited to the case of an embedded crack in an infinite body with a relatively simple load, many numerical methods have been developed, such as the finite element method (FEM), the Schwartz alternating technique combined with the finite element method, the boundary element method (BEM), and so on. Among these methods, the FEM is relatively expensive and has poor precision, and the BEM has the advantage of simpler discretization and inexpensiveness. Cruse and Vanburen solved 3-D crack problems using the constant boundary element method as early as 1971 (Cruse and Vanburen, 1971). Later, the BEM has been widely used and developed. For instance, Jia and Shippy et al. analyzed the crack problems by using the singular boundary element method (Jia et al., 1989), and they applied the $\sqrt{r}$ displacement and $1/\sqrt{r}$ traction behaviors near the crack front and presented a multi-domain approach to the solution to the problem of an infinite elastic body containing a planar crack. Levan and Peseux proposed a principal value integral equation using a tensor formalism for flat cracks, and presented a discretization with no actual principal value computation (Levan and Peseux, 1988). Although the BEM has many advantages, it is still difficult to solve crack problems using only the BEM. Due to Ioakimidis (1982), the hypersingular integral equation has been applied to fracture mechanics. It has been well recognized that this method has great power in solving linear elastic crack problems in infinite elastic bodies. The general advantage of this approach is that arbitrary shaped cracks under arbitrary distributed crack-face tractions can be conveniently treated through numerical integration over the crack surface. Therefore, the hypersingular integral equation approach has been widely used and developed by many authors. Takakuda et al. derived

the hypersingular integral equations of a flat crack in an infinite body for normal and shear tractions (1985). Lin'kov and Mogilevshaya achieved the analogous equations too (1986). Mayrhofer and Fischer have given an analytical solution for a two-dimensional hypersingular integral equation (1992), but their solution is limited to elliptical crack problems. Sohn and Hong treated crack problems in an infinite body through solving these equations, and solved several crack problems in a finite body by using the finite-part integral method combined with the Schwarz alternating method (Sohn and Hong, 1985) and also employed the displacement behaviors on the crack-front elements (Sohn and Hong, 1992), but they assumed that the displacements in these special elements vary only linearly along the crack-front direction and vary in $\sqrt{r}$ behavoir in the direction normal to the crack front. Tang and Qin proved strictly Takakuda's equations and that the unknowns near the crack front have the square root behavior. Moreover, they accurately derived the singular stresses near the smooth point of the crack front (Tang and Qin, 1993).

In this paper, based on our work (Qin and Tang, 1993), a set of hypersingular integral equations to solve planar crack problems in three-dimensional finite elastic solids subjected to arbitrary loads is derived, and its numerical method is presented. According to the analytical theory (Tang and Qin, 1993), the square root models of the displacement discontinuities in elements near the crack front are employed, and thus the numerical approach given by paper (Qin and Tang, 1993) is improved. The stress intensity factor numerical solutions to several typical crack problems are given in the last section.

2. Basic formulae and integral equations for a planar crack in a finite body

2.1. Components of displacement and stress

Consider a planar crack $S(S^{\pm})$ of arbitrary shape inside a finite body. Suppose that x_1 and x_2 are Cartesian coordinates in the crack plane and x_3 is normal to the crack. Using the Somigliana representation, the displacements at an internal point p can be expressed as follows (Cruse and Vanburen, 1971)

$$\begin{aligned} u_k(p) \;=\; & -\int_\Gamma T_{ki}(p,Q)u_i(Q)\,\mathrm{d}s(Q) + \int_\Gamma U_{ki}(p,Q)t_i(Q)\,\mathrm{d}s(Q) \\ & - \int_{S^+} T^+_{ki}(p,Q)\tilde{u}_i(Q)\,\mathrm{d}s(Q), \\ & p \in \Omega; \quad k,i = 1,2,3, \end{aligned} \tag{2.1}$$

where u_i and t_i are displacement and traction boundary values respectively, $\tilde{u}_i = u_i^+ - u_i^-$ is the ith displacement discontinuity of the crack $S, T^+_{ki}(p,Q)$ is the value of $T_{ki}(p,Q)$ at point $Q \in S^+$, and $U_{ki}(p,Q)$ and $T_{ki}(p,Q)$ are Kelvin's point force solutions of three-dimensional elastostatics

$$U_{ki}(p,Q) = \frac{1+v}{8\pi E(1-v)r}[(3-4v)\delta_{ki} + r_{,k}r_{,i}], \tag{2.2}$$

$$\begin{aligned} T_{ki}(p,Q) \;=\; & -\frac{1}{8\pi(1-v^2)r^2} \\ & \times \left\{ \frac{\partial r}{\partial n}[(1-2v)\delta_{ki} + 3r_{,k}r_{,i}] - (1-2v)(r_{,k}n_i - r_{,i}n_k) \right\}, \end{aligned} \tag{2.3}$$

in which v is Poisson's ratio, E is the elastic modulus, r is the distance between point p to boundary point Q.

Using the displacement expression (2.1) and the constitutive relations, the corresponding stresses at point p are obtained

$$\begin{aligned}\sigma_{ij}(p) \;=\; & -\int_\Gamma S_{kij}(p,Q)u_k(Q)\,\mathrm{d}s(Q) + \int_\Gamma D_{kij}(p,Q)t_k(Q)\,\mathrm{d}s(Q) \\ & -\int_{S^+} S^+_{kij}(p,Q)\tilde{u}_k(Q)\,\mathrm{d}s(Q), \quad p\in\Omega; \quad k,i=1,2,3,\end{aligned} \tag{2.4}$$

where $S^+_{kij}(p,Q)$ is the value of $S_{kij}(p,Q)$ at point $Q\in S^+$, and the integral kernels S_{kij} and D_{kij} are

$$\begin{aligned}S_{kij} \;=\; & \frac{E}{8\pi(1-v^2)r^3} \\ & \times\Big\{3\frac{\partial r}{\partial n}[(1-2v)r_{,k}\delta_{ij}+v(r_{,i}\delta_{jk}+r_{,j}\delta_{ik})-3rt_{,k}r_{,i}r_{,j}]+3v(r_{,i}n_j+r_{,j}n_i)r_k \\ & +(1-2v)(3r_{,i}r_{,j}n_k+n_i\delta_{jk}+n_j\delta_{ik})-(1-4v)n_k\delta_{ij}\Big\}\end{aligned} \tag{2.5}$$

$$D_{kij} = \frac{1}{8\pi(1-v^2)r^2}[(1-2v)(r_{,i}\delta_{jk}+r_{,j}\delta_{ik}-r_{,k}\delta_{ij})+3r_{,k}r_{,i}r_{,j}]. \tag{2.6}$$

2.2. HYPERSINGULAR INTEGRAL EQUATIONS

The integral equations for the crack problems can be written as (Cruse and Vanburen, 1971; Takakuda et al., 1985)

$$\begin{aligned}&\frac{E}{8\pi(1-v^2)}\oint\!\!\!\!\!\!=_{S^+}\frac{1}{r^3}[(1-2v)\delta_{\alpha\beta}+3vr_{,\alpha}r_\beta]\tilde{u}_\beta\,\mathrm{d}\xi_1\,\mathrm{d}\xi_2 \\ &\quad -\int_\Gamma S_{k\alpha3}(p,Q)u_k(Q)\,\mathrm{d}s(Q) \\ &\quad =-\int_\Gamma D_{k\alpha3}(p,Q)t_k(Q)\,\mathrm{d}s(Q), \quad P\in S^+; \quad \alpha,\beta=1,2,\end{aligned} \tag{2.7}$$

$$\begin{aligned}&\frac{E}{8\pi(1-v^2)}\oint\!\!\!\!\!\!=_{S^+}\frac{1}{r^3}\tilde{u}\,\mathrm{d}\xi_1\,\mathrm{d}\xi_2-\int_\Gamma S_{k33}(p,Q)u_k(Q)\,\mathrm{d}s(Q) \\ &\quad =-\int_\Gamma D_{k33}(p,Q)t_k(Q)\,\mathrm{d}s(Q), \quad P\in S^+,\end{aligned} \tag{2.8}$$

$$\begin{aligned}&c_{ki}u_i(P)+\int_\Gamma T_{ki}(P,Q)u_i(Q)\,\mathrm{d}s(Q)+\int_{S^+}T^+_{ki}(P,Q)\tilde{u}_i(Q)\,\mathrm{d}s(Q) \\ &\quad =\int_\Gamma U_{ki}(P,Q)t_i(Q)\,\mathrm{d}s(Q), \quad P\in\Gamma,\end{aligned} \tag{2.9}$$

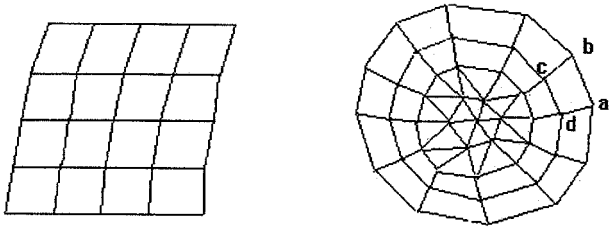

Figure 1. (a) Element mesh of part of boundary Γ; (b) Element mesh of crack surface S.

where $\oint\!\!\!\!\!\!-$ is the symbol of the finite-part integral, c_{ki} is the constant related to the boundary point P. Notice that Equations (2.7∼2.8) are hypersingular integral equations, and (2.9) is the general boundary integral equation. Simultaneously solving these equations, we can obtain all the displacement discontinuities $\tilde{u}_i (i = 1, 2, 3)$, from which the stress intensity factors can be calculated.

3. Numerical technique

Equations (2.7∼2.9) are hypersingular integral equations coupled with the boundary integral equation, and can be numerically solved by use of the boundary element method combined with the finite-part integral method. Assuming that the crack surface S^+ and the boundary Γ are divided into a number of elements as shown in Figure 1, Equations (2.7∼2.9) can be reduced to a set of linear algebraic equations, which can be expressed in a matrix form as

$$\mathbf{A} \cdot \{\tilde{u}_i\} + \mathbf{B} \cdot \{u_i\} = \mathbf{C} \cdot \{t_i\}, \quad P_n \in S^+, \tag{3.1}$$

$$\mathbf{D} \cdot \{\tilde{u}_i\} + \mathbf{H} \cdot \{u_i\} = \mathbf{G} \cdot \{t_i\}, \quad P_n \in \Gamma, \tag{3.2}$$

where P_n are the nodal points of S^+ or Γ, $\{\tilde{u}_i\}$ is the vector of the displacement discontinuities at all the nodal points of S^+, $\{u_i\}$ and $\{t_i\}$ are the vectors of the boundary displacements and tractions respectively at all the nodal points of Γ, and **A**, **B**, **C**, **D**, **G** and **H** are the coefficient matrix whose components are integrals over each element. Now the main task is to numerically calculate these integrals.

The integrals over the elements of boundary Γ can be evaluated by the general boundary element method. To improve the numerical solution precision, the elements of S^+ are divided into two groups. One is the crack-front element group which is joined with the crack front, and the other is the internal element group. The integrals over the latter elements can be calculated as in paper (Qin and Tang, 1993). In this paper, we only treat the integrals over the crack-front elements. Among these integrals, there are not only general integrals, but also hypersingular integrals. For the sake of convenience, it is assumed that the crack-front elements are rectangular elements (triangular elements can be analogously treated), and their internal sides parallel to the sides on the crack front (such as $cd//ab$ in Figure 1(b)). If the reference point is not in the integrating element, the integrals are normal, and $\tilde{u}_i$ is assumed as follows

$$\tilde{u}_i = \sqrt{\frac{1-\xi}{2}}[\tfrac{1}{4}(1-\xi)(1-\eta)\tilde{u}_i^{(d)} + \tfrac{1}{4}(1-\xi)(1+\eta)\tilde{u}_i^{(c)} + \tfrac{1}{4}(1+\xi)(1-\eta)\sqrt{D}c_i^{(a)}$$
$$\tfrac{1}{4}(1+\xi)(1+\eta)\sqrt{D}c_i^{(b)}], \tag{3.3}$$

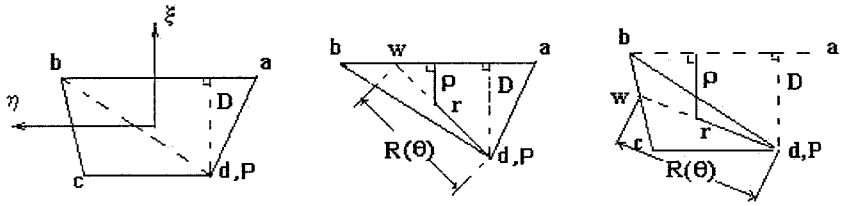

Figure 2. Crack-front element.

where (ξ, n) are the local dimensionless coordinates as shown in Figure 2(a), $c_i^{(a)}$ and $c_i^{(b)}$ are unknown constants related to the crack-front point a and b respectively, and D is the distance between side cd and side ab. The relative integrals can be calculated as normal one. It is noticed that $\tilde{u}_i$ defined by (3.3) has the $\sqrt{r}$ behavior near the crack front, which is consistent with the analytical theory [10]. If the reference point coincides with one of the nodes of the integrating element, the integrals are hypersingular, which can be written as follows

$$I_m = \oint\!\!\!\!\!\!= \int_{S_m} \frac{1}{r^3}[(1-2v)\delta_{\alpha\beta} + 3v r_{,\alpha} r_{,r\beta}]\tilde{u}_\beta \xi_1 \,\mathrm{d}\xi_2, \tag{3.4}$$

$$I_m = \oint\!\!\!\!\!\!= \int_{S_m} \frac{1}{r^3}\tilde{u}_3 \,\mathrm{d}\xi_1 \,\mathrm{d}\xi_2. \tag{3.5}$$

These hypersingular integrals must be specially treated, and the computing technique will be given. First, it is assumed that the reference point P coincides with the internal point d. Linking point d with b, the element is divided into two triangular elements S_{m1} and S_{m2} as shown in Figure 2(a). The displacement discontinuities can be expressed as

$$\tilde{u}_i = \sqrt{\frac{\rho}{D}}[L_d \tilde{u}_i^{(d)} + L_a\sqrt{D}c_i^{(a)} + L_b\sqrt{D}c_i^{(b)}], \quad Q \in S_{m1}, \tag{3.6}$$

$$\tilde{u}_i = \sqrt{\frac{\rho}{D}}[L_d \tilde{u}_i^{(d)} + L_c \tilde{u}_i^{(c)} + L_b\sqrt{D}c_i^{(b)}], \quad Q \in S_{m2}, \tag{3.7}$$

where L_a, L_b, L_c, and L_d are the area coordinates of S_{m1} and S_{m2} respectively, ρ is the perpendicular distance from the integrating point Q to the crack front ab, and can be determined as follows

$$\rho = \left(1 - \frac{r}{R}\right) D, \quad Q \in S_{m1} \tag{3.8}$$

$$\rho = \left[1 - (1 - S_c)\frac{r}{R}\right] D, \quad Q \in S_{m2}, \tag{3.9}$$

in which S_c is the area coordinate of point w, and R is the distance between point d and point w. The hypersingular integrals related to (3.6) can be written as

$$I_{dd} = \oint\!\!\!\!\!\!= \int_{S_{m1}} \frac{1}{r^3}[(1-2v)\delta_{\alpha\beta} + 3v r_{,\alpha} r_{,\beta}]\sqrt{1 - \frac{r}{R}} L_d \,\mathrm{d}\xi_1 \,\mathrm{d}\xi_2$$

$$= \oint\!\!\!\!\!\!-_{S_{m1}} \frac{1}{r^3}[(1-2v)\delta_{\alpha\beta} + 3vr_{,\alpha}r_{,\beta}]\sqrt{1-\frac{r}{R}}\left(1-\frac{r}{R}\right)\,\mathrm{d}\xi_1\,\mathrm{d}\xi_2$$

$$= \int_\alpha [(1-2v)\delta_{\alpha\beta} + 3vR_{,\alpha}R_{,\beta}]\,\mathrm{d}\theta \oint\!\!\!\!\!\!-_0^{R(\theta)} \frac{1}{r_2}\sqrt{1-\frac{r}{R}}\left(1-\frac{r}{R}\right)\,\mathrm{d}r$$

$$= 3\Delta(1-2\ln 2)\int_0^1 \frac{1}{R^3(\theta)}[(1-2v)\delta_{\alpha\beta} + 3vR_{,\alpha}R_{,\beta}]\,\mathrm{d}S_b, \tag{3.10}$$

$$I_{da} = \sqrt{D}\oint\!\!\!\!\!\!-_{S_{m1}} \frac{1}{r^3}[(1-2v)\delta_{\alpha\beta} + 3vr_{,\alpha}r_{,\beta}]\sqrt{1-\frac{r}{R}}L_a\,\mathrm{d}\xi_1\,\mathrm{d}\xi_2$$

$$= \sqrt{D}\oint\!\!\!\!\!\!-_{S_{m1}} \frac{1}{r^3}[(1-2v)\delta_{\alpha\beta} + 3vr_{,\alpha}r_{,\beta}]\sqrt{1-\frac{r}{R}}(1-S_b)\frac{r}{R}\,\mathrm{d}\xi_1\,\mathrm{d}\xi_2$$

$$= \sqrt{D}\int_\alpha \frac{1}{R(\theta)}(1-S_b)[(1-2v)\delta_{\alpha\beta} + 3vR_{,\alpha}R_{,\beta}]\,\mathrm{d}\theta \oint\!\!\!\!\!\!-_0^{R(\theta)} \frac{1}{r}\sqrt{1-\frac{r}{R}}\,\mathrm{d}r$$

$$= -4\Delta(1-\ln 2)\sqrt{D}\int_0^1 \frac{1}{R^3(\theta)}[(1-2v)\delta_{\alpha\beta} + 3vR_{,\alpha}R_{,\beta}](1-S_b)\,\mathrm{d}S_b, \tag{3.11}$$

$$I_{da} = \sqrt{D}\oint\!\!\!\!\!\!-_{S_{m1}} \frac{1}{r^3}[(1-2v)\delta_{\alpha\beta} + 3vr_{,\alpha}r_{,\beta}]\sqrt{1-\frac{r}{R}}L_b\,\mathrm{d}\xi_1\,\mathrm{d}\xi_2$$

$$= \sqrt{D}\oint\!\!\!\!\!\!-_{S_{m1}} \frac{1}{r^3}[(1-2v)\delta_{\alpha\beta} + 3vr_{,\alpha}r_{,\beta}]\sqrt{1-\frac{r}{R}}S_b\frac{r}{R}\,\mathrm{d}\xi_1\,\mathrm{d}\xi_2$$

$$= \sqrt{D}\int_\alpha \frac{1}{R(\theta)}S_b[(1-2v)\delta_{\alpha\beta} + 3vR_{,\alpha}R_{,\beta}]d\theta \oint\!\!\!\!\!\!-_0^{R(\theta)} \frac{1}{r}\sqrt{1-\frac{r}{R}}\,\mathrm{d}r$$

$$= -4\Delta(1-\ln 2)\sqrt{D}\int_0^1 \frac{1}{R^3(\theta)}[(1-2v)\delta_{\alpha\beta} + 3vR_{,\alpha}R_{,\beta}]S_b\,\mathrm{d}S_b, \tag{3.12}$$

where Δ is the area of element S_{m1}, $\oint\!\!\!\!\!\!-$ is the symbol of the principal-value integral, and S_b is the area coordinate of point w on the side ab. The hypersingular integrals related to (3.7) can be analogously treated, here we only give the computing formula for the first one

$$I_{dd} = \oint\!\!\!\!\!\!-_{S_{m2}} \frac{1}{r^3}[(1-2v)\delta_{\alpha\beta} + 3vr_{,\alpha}r_{,\beta}]\sqrt{1-(1-S_c)\frac{r}{R}}L_d\,\mathrm{d}\xi_1\,\mathrm{d}\xi_2$$

$$= 2\Delta\int_0^1 \frac{1}{R^3(\theta)}[(1-2v)\delta_{\alpha\beta} + 3vR_{,\alpha}R_{,\beta}]$$

$$\times\left[\tfrac{1}{2}(3+S_c) - 3\sqrt{S_c} + (3-S_c)\ln\frac{1+\sqrt{S_c}}{2}\right]\mathrm{d}S_c. \tag{3.13}$$

Second, if the reference point P infinitely tends to crack-front point a, link point a with c, and the element is divided into two triangular elements S_{m1} and S_{m2} as shown in Figure 3. The displacement discontinuities can be expressed as

$$\tilde{u}_i = \sqrt{\frac{\rho}{D}}[L_c\tilde{u}_i^{(d)} + L_a\sqrt{D}c_i^{(a)} + L_b\sqrt{D}c_i^{(b)}], \quad Q \in S_{m1}, \tag{3.14}$$

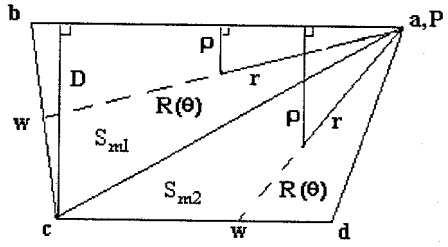

Figure 3. Crack-front element.

$$\tilde{u}_i = \sqrt{\frac{\rho}{D}}[L_c\tilde{u}_i^{(c)} + L_d\tilde{u}_i^{(d)} + L_a\sqrt{D}c_i^{(a)}], \quad Q \in S_{m2}, \tag{3.15}$$

where ρ can be determined as follows

$$\rho = \frac{r}{R}DS_c, \quad \rho \in S_{m1}, \tag{3.16}$$

$$\rho = \frac{r}{R}D, \quad \rho \in S_{m2}, \tag{3.17}$$

The hypersingular integrals related to (3.14) can be written as

$$\begin{aligned} I_{aa} &= \sqrt{D}\oint_{S_{m1}} \frac{1}{r^3}[(1-2v)\delta_{\alpha\beta} + 3vr_{,\alpha}r_{,\beta}]\sqrt{\frac{r}{R}S_c}L_a \,\mathrm{d}\xi_1\,\mathrm{d}\xi_2 \\ &= \sqrt{D}\int_\alpha [(1-2v)\delta_{\alpha\beta} + 3vR_{,\alpha}R_{,\beta}]\sqrt{S_c}\,\mathrm{d}\theta \oint_0^{R(\theta)} \frac{1}{r^2}\sqrt{\frac{r}{R}}\left(1-\frac{r}{R}\right)\mathrm{d}r \\ &= -8\Delta\sqrt{D}\int_0^1 \frac{1}{R^3(\theta)}[(1-2v)\delta_{\alpha\beta} + 3vR_{,\alpha}R_{,\beta}]\sqrt{S_c}\,\mathrm{d}S_c, \end{aligned} \tag{3.18}$$

$$\begin{aligned} I_{ab} &= \sqrt{D}\oint_{S_{m1}} \frac{1}{r^3}[(1-2v)\delta_{\alpha\beta} + 3vr_{,\alpha}r_{,\beta}]\sqrt{\frac{r}{R}S_c}L_a \,\mathrm{d}\xi_1\,\mathrm{d}\xi_2 \\ &= \sqrt{D}\int_\alpha [(1-2v)\delta_{\alpha\beta} + 3vR_{,\alpha}R_{,\beta}](1-S_c)\sqrt{S_c}\,\mathrm{d}\theta \oint_0^{R(\theta)} \frac{1}{rR}\sqrt{\frac{r}{R}}\,\mathrm{d}r \\ &= 4\Delta\sqrt{D}\int_0^1 \frac{1}{R^3(\theta)}[(1-2v)\delta_{\alpha\beta} + 3vR_{,\alpha}R_{,\beta}]\sqrt{S_c}(1-S_c)\,\mathrm{d}S_c, \end{aligned} \tag{3.19}$$

$$\begin{aligned} I_{ac} &= \oint_{S_{m1}} \frac{1}{r^3}[(1-2v)\delta_{\alpha\beta} + 3vr_{,\alpha}r_{,\beta}]\sqrt{\frac{r}{R}S_c}L_c \,\mathrm{d}\xi_1\,\mathrm{d}\xi_2 \\ &= \int_\alpha S_c^{3/2}[(1-2v)\delta_{\alpha\beta} + 3vR_{,\alpha}R_{,\beta}]\,\mathrm{d}\theta \oint_0^{R(\theta)} \frac{1}{rR}\sqrt{\frac{r}{R}}\,\mathrm{d}r \\ &= 4\Delta\int_0^1 \frac{1}{R^3(\theta)}[(1-2v)\delta_{\alpha\beta} + 3vR_{,\alpha}R_{,\beta}]S_c^{3/2}\,\mathrm{d}S_c. \end{aligned} \tag{3.20}$$

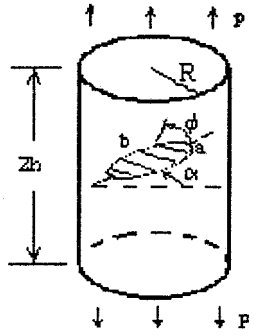

Figure 4. An elliptical crack in a cylinder.

The hypersingular integrals related to (3.15) can be analogously treated, here we only give the computing formula for the first one

$$I_{aa} = \oint\!\!\!\!\!\!= \int_{S_{m2}} \frac{1}{r^3}[(1-2v)\delta_{\alpha\beta} + 3vr_{,\alpha}r_{,\beta}]\sqrt{\frac{r}{R}}DL_a \,\mathrm{d}\xi_1\,\mathrm{d}\xi_2$$

$$= -8\Delta\sqrt{D}\int_0^1 \frac{1}{R^3(\theta)}[(1-2v)\delta_{\alpha\beta} + 3vR_{,\alpha}R_{,\beta}]\,\mathrm{d}S_d. \tag{3.21}$$

If the reference point P coincides with point c or infinitely tends to point b, the related hypersingular integrals can be analogously treated as above. After computing the integrals over all the elements, Equations (3.1∼3.2) can now be solved, and then all the nodal values of $\tilde{u}_i$ and c_i are known, from which the stress intensity factors at point Q_0 on the crack front ab can be calculated as follows

$$K_{\mathrm{I}}(Q_0) = \frac{E}{8(1-v^2)} \lim_{Q\to Q_0} \tilde{u}_3(Q)\cdot(2/\rho)^{1/2} = \frac{E}{8(1-v^2)}\sqrt{2}[S_a c_3^{(a)} + S_b c_3^{(b)}], \tag{3.22}$$

$$K_{\mathrm{II}}(Q_0) = \frac{E}{8(1-v^2)} \lim_{Q\to Q_0} \tilde{u}_n(Q)\cdot(2/\rho)^{1/2} = \frac{E}{8(1-v^2)}\sqrt{2}[S_a c_n^{(a)} + S_b c_n^{(b)}], \tag{3.23}$$

$$K_{\mathrm{III}}(Q_0) = \frac{E}{8(1+v)} \lim_{Q\to Q_0} \tilde{u}_\tau(Q)\cdot(2/\rho)^{1/2} = \frac{E}{8(1+v)}\sqrt{2}[S_a c_\tau^{(a)} + S_b c_\tau^{(b)}], \tag{3.24}$$

where $(3, n, \tau)$ are the local coordinates, S_a and S_b are the area coordinates of point Q_0 of Δabd.

4. Numerical results

In order to verify the above method and illustrate its application, numerical calculations are performed for a crack embedded in a finite body.

4.1. Elliptical crack embedded in a cylinder under tension

Let us consider an elliptical crack embedded in a circular cylinder. The crack is inclined to the center symmetric plane of the cylinder with angle α as shown in Figure 4, and the cylinder

Table 1. Stress intensity factors $K_{\mathrm{I}}/K_{\mathrm{I}}^0$ ($h/R = 1, a/b = 1, \alpha = 0$)

a/R	0.25	0.5	0.75
Yamamoto		1.114	1.402
Nishioka		1.111	1.410
Sohn			1.39
present	1.020	1.109	1.389

is subjected to tension load. In the case of a circular crack and the crack being symmetrically located at the center plane of the cylinder, i.e. $a/b = 1$ and $\alpha = 0$, there is only mode **I** of the stress intensity factors, and the dimensionless stress intensity factors are listed in Table 1, where K_{I}^0 is the stress intensity factor for a penny-shaped crack in an infinite body under constant pressure. It is observed that present results are close to other results obtained by Yamamoto and Sumi (1973) by the axisymmetric finite element method, Nishioka and Atluri (1983) by the Schwartz alternating technique in conjunction with the finite element method, and Sohn and Hong (1985) by the finite alternating method combined with the finite-part integral method.

In general, when the crack is inclined and the cylinder is subjected to tension load, there are three different modes of stress intensity factors, i.e. mode **I** $K_{\mathrm{I}}(\phi)$, mode **II** $K_{\mathrm{II}}(\phi)$ and mode **III** $K_{\mathrm{III}}(\phi)$, and their dimensionless values $K_{\mathrm{I}}^* = K_{\mathrm{I}}(\phi)/p\sqrt{b}, K_{\mathrm{II}}^* = K_{\mathrm{II}}(\phi)/p\sqrt{b}$, and $K_{\mathrm{III}}^* = K_{\mathrm{III}}(\phi)/p\sqrt{b}$ are graphically shown in Figure 5(a), Figure 5(b), and Figure 5(c), respectively. Obviously, when the crack is located at the center plane of the cylinder, $\alpha = 0$ i.e., there is only mode **I** of stress intensity factor.

4.2. Elliptical crack embedded in a cylinder under tension and bending

Assuming that there is an elliptical crack in the center of a cylinder as shown in Figure 6(a), its major axis and minor axis are a and b respectively, and the radius of the cylinder is R. As the cylinder is subjected to a coupled load of tension and bending, i.e., the upper base surface is under linearly varying traction: $t_3 = p(1 + x_1/R)$, the numerical results of the dimensionless stress intensity factors $K_{\mathrm{I}}^* = K_{\mathrm{I}}(\phi)/p\sqrt{b}$ are given in Figure 6(b). It is shown that the maximum value of the stress intensity factors for an elliptical crack occurs at the crack-front point near the major axis that is subjected to the largest load. In the case of a circular crack and $h/R = 3$, Nishioka and Atluri [13] obtained the maximum value of the stress intensity factors as $(K_{\mathrm{I}})_{\max} = 1.114p\sqrt{a}$, which differs by 6 % from the present case in which $h/R = 1$.

4.3. Elliptical crack embedded in a cylinder under torsion

The configuration and geometrical parameters of a cylinder with an embedded elliptical crack are the same as shown in Figure 6(a). When the cylinder is under torsion, i.e., the upper base surface is subjected to radial-directional shear traction: $t_\theta = qr/R$, there are two different modes of stress intensity factors along the crack front, i.e., mode **II** $K_{\mathrm{II}}(\phi)$ and mode **III** $K_{\mathrm{III}}(\phi)$, and their dimensionless values $K_{\mathrm{II}}^* = K_{\mathrm{II}}(\phi)/p\sqrt{b}$ and $K_{\mathrm{III}}^* = K_{\mathrm{III}}(\phi)/p\sqrt{b}$ are

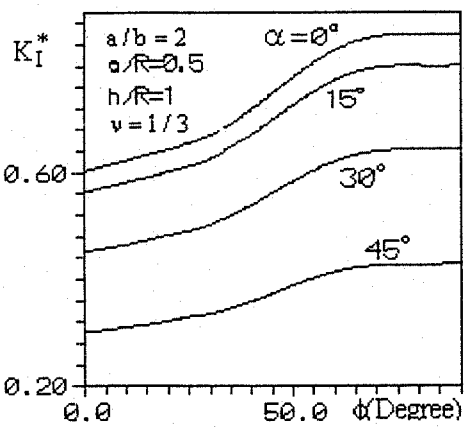

Figure 5a. Stress intensity factor K_{I}.

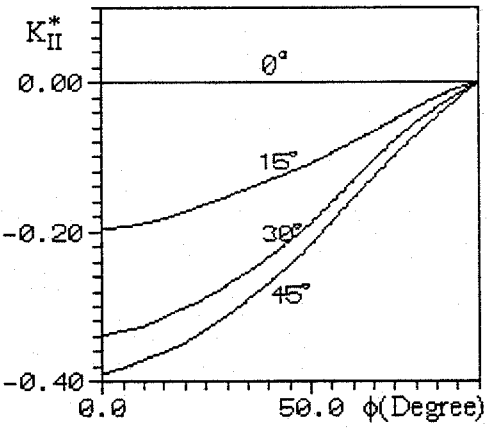

Figure 5b. Stress intensity factor K_{II}.

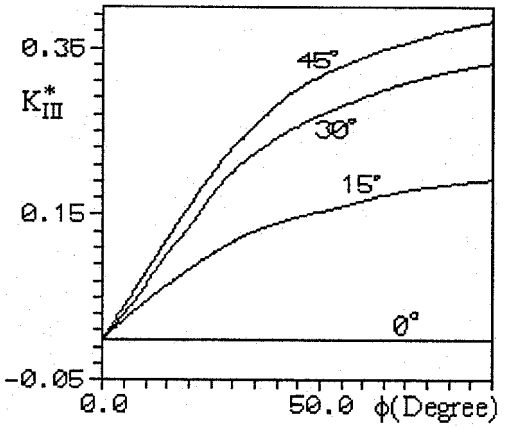

Figure 5c. Stress intensity factor K_{III} for an elliptical crack in a cylinder under tension.

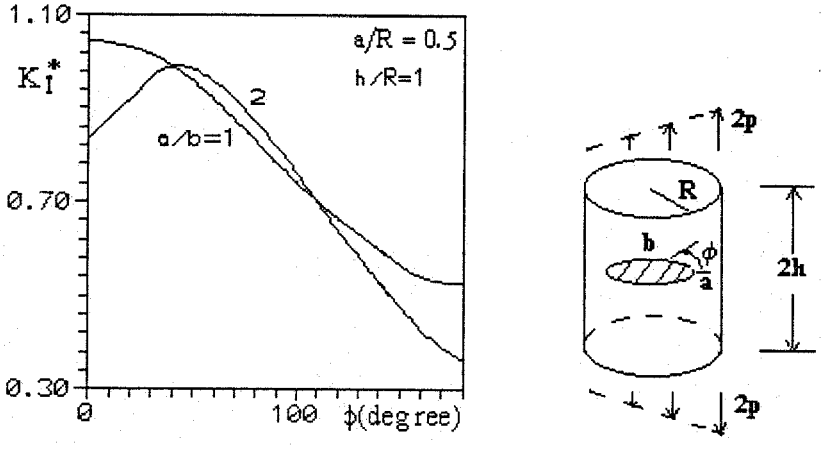

Figure 6. (a) An elliptical crack in a cylinder; (b) Dimensionless stress intensity factors.

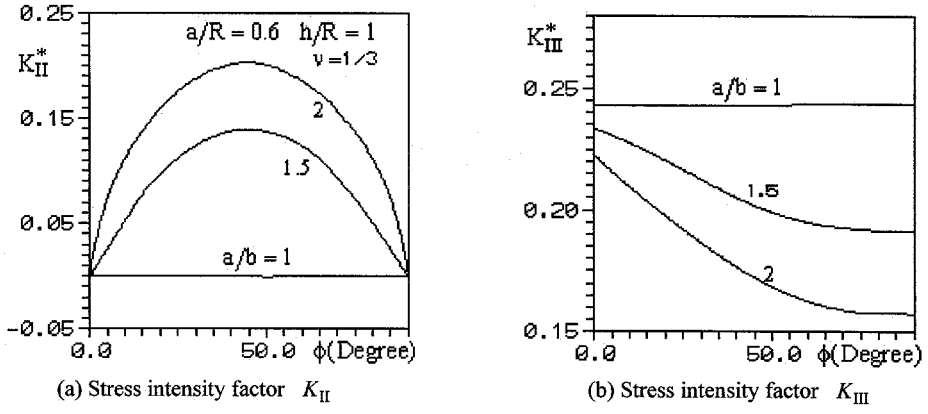

Figure 7. Stress intensity factors for an elliptical crack in a cylinder under torsion.

graphically shown in Figure 7(a) and Figure 7(b), respectively. It is shown that there is only a mode **III** stress intensity factor along the crack front for a penny-shaped crack.

5. Conclusions

In the present paper, three-dimensional crack problems in a finite elastic solid subjected to arbitrary loads are investigated by using the hypersingular integral equation method, and the numerical technique proposed by the boundary element method combined with the finite-part integral method improves the one described in paper (Qin and Tang, 1993). The advantage of this numerical technique is that it applies the square root behavior of the displacement discontinuities near the crack front and enables the stress intensity factors to be directly calculated. Such square root models in the elements near the crack front are tested. The results show that this technique is successful, and the solution precision is satisfied.

The present study is limited to embedded planar crack problems. However, the present numerical technique can be extended to solve the 3-D surface crack problems and other complex crack problems.

References

Cruse, T.A. and Vanburen, W. (1971). Three-dimensional elastic stress analysis of a fracture specimen with an edge crack. *International Journal of Fracture* **17**, 1–15.

Ioakimidis, N.I. (1982). Application of finite-part integrals to the singular integral equations of crack problems in plane and three-dimensional elasticity. *Acta Mechanica* **45**, 31–47.

Jia, Z.H., Shippy, D.J. and Rizzo, F.J. (1989). Three-dimensional crack analysis using singular boundary elements. *International Journal for Numerical Methods in Engineering* **28**, 2257–2273.

Levan, A. and Peseux, B. (1988). Boundary element analysis of an integral equation for three-dimensional crack problems. *International Journal for Numerical Methods in Engineering* **26**, 2383–2402.

Lin'kov, A.M. and Mogilevshaya, S.G. (1986). Finite-part integral in problems of three-dimensional cracks. *Journal of Applied Mathematics and Mechanics (PPM)* **50**, 652–658.

Mayrhofer, K. and Fischer, F.D. (1992). Derivation of a new analytical solution for a general two-dimensional finite-part integral applicable in fracture mechanics. *International Journal for Numerical Methods in Engineering* **33**, 1027–1047.

Nishioka, T. and Atluri, S.N. (1983). Analytical solution for embedded elliptical cracks, and finite element alternating method for elliptical surface cracks, subjected to arbitrary loadings. *Engineering Fracture Mechanics* **171**, 247–268.

Qin, T.Y. and Tang, R.J. (1993). Finite-part integral and boundary element method to solve embedded planar crack problems. *International Journal of Fracture* **60**, 373–381.

Sohn, G.H. and Hong, C.S. (1985) Application of singular integral equations to embedded planar crack problems in finite body. *Boundary Element*, Vol.2 (Edited by A.C. Brebbia and G. Maier), Springer-Verlag, Berlin, 8–57, 8–67.

Sohn, G.H. and Hong, C.S. (1992). Determination of three-dimensional stress intensity factor using virtual crack extension technique based on singular integral equations. *Engineering Fracture Mechanics* **41**, 177–190.

Takakuda, K., Koizumi, T. and Shibuya, T. (1985). On integral equation methods for the crack problems. *Bulletin of the Japan Society of Precision Engineering* **28**, 217–224.

Tang, R.J. and Qin, T.Y. (1993). Method of hypersingular integral equations for three-dimensional. *Acta Mechanica Sinica* **25**, 665–675.

Yamamoto, Y. and Sumi, Y. (1973). Stress intensity factors in a cracked axisymmetric body calculated by the finite element method. *Journal Society Naval Architects of Japan* **133**, 179–187.